J Rep Pharm Sci. 2024 December; 12(1): e145411 https://doi.org/10.5812/jrps-145411

Published Online: 2024 December 2 **Research Article**

Assessment of Punicalagin Activity Against Influenza A Virus Proteins via In-silico Approaches

Majid Asadi-Samani [1], Dhiya Altememy [2], Javad Saffari-Chaleshtori [3,**], Mohammad-Taghi Moradi [4,*]

[1] Cellular and Molecular Research Center, Basic Health Sciences Institute, Shahrekord University of Medical Sciences, Shahrekord, Iran
[2] Department of Pharmaceutics, College of Pharmacy, Al-Zahraa University for Women, Karbala, Iraq
[3] Clinical Biochemistry Research Center, Basic Health Sciences Institute, Shahrekord University of Medical Sciences, Shahrekord, Iran
[4] Basic Health Sciences Institute, Shahrekord University of Medical Sciences, Shahrekord, Iran

[*] ***Corresponding Author:*** Basic Health Sciences Institute, Shahrekord University of Medical Sciences, Shahrekord, Iran. Email: mtmoradi65@gmail.com
[**] ***Corresponding Author:*** Clinical Biochemistry Research Center, Basic Health Sciences Institute, Shahrekord University of Medical Sciences, Shahrekord, Iran. Email: j_saffari@yahoo.com

Received: 4 February, 2024; **Revised:** 19 October, 2024; **Accepted:** 26 October, 2024

Abstract

Background: To investigate the anti-influenza mechanism of punicalagin and its inhibitory effects on influenza virus proteins, we conducted molecular docking studies targeting 11 viral proteins. Additionally, molecular dynamics simulations were performed for the protein with the lowest free energy and the minimum concentration required for binding in a simulated environment.

Methods: The molecular structure and data of punicalagin were obtained from the PubChem database and converted into a PDB file. FASTA sequences of viral proteins were retrieved from UniProt, and their PDB structures were predicted using the I-TASSER server. Molecular docking was performed using AutoDock 4.2 software, while molecular dynamics simulations were conducted with Gromacs 2022 software.

Results: The PB1-F2 protein exhibited the best inhibitory performance, with a binding energy of -5.76 kcal/mol and the lowest inhibition constant (Ki). Docking of punicalagin to the PB1-F2 protein led to a significant decrease in the average total energy (TE), radius of gyration (Rg), and root mean square deviation (RMSD), as well as alterations in the secondary structure of the protein ($P < 0.001$). The most prominent secondary structural change was a reduction in coil structures and an increase in turn structures.

Conclusions: Punicalagin displayed a strong binding affinity for the PB1-F2 protein compared to other influenza viral proteins. Considering the role of PB1-F2 in exacerbating inflammation caused by influenza, punicalagin may mitigate inflammation in patients by modulating the activity of this protein.

Keywords: Influenza, Anti-inflammatory Agents, Molecular Docking, Molecular Dynamics Simulation

1. Background

Influenza A is a viral respiratory illness that can lead to pneumonia and severe complications, including acute respiratory distress syndrome. It is responsible for an annual global mortality rate of approximately 290,000 to 650,000 individuals and is known to induce alterations in the secondary structure of proteins (1). The genome of Influenza A consists of a single-stranded RNA molecule with a negative-sense orientation, segmented into eight distinct parts. These segments encode proteins essential for viral replication and pathogenicity (2, 3).

The first three segments and the fifth segment encode components of the viral replication machinery, including nucleoprotein (NP), polymerase A protein (PA), polymerase B1 protein (PB1), and polymerase B2 protein (PB2). Additionally, some strains encode the PB1-F2 protein within the PB1 segment. The fourth and sixth segments encode neuraminidase and hemagglutinin, the surface glycoproteins of the virus. The seventh segment encodes the M1 and M2 proteins, while the smallest segment, NS, encodes the NS1 protein (an

interferon antagonist) and NS2 protein from spliced and unspliced mRNA transcripts (4).

In recent decades, several antiviral agents have been developed to treat influenza, including RNA polymerase inhibitors (e.g., Fluorodeoxyuridine analogues, Favipiravir), neuraminidase inhibitors (e.g., Zanamivir, Oseltamivir, Laninamivir, Peramivir), and M2 ion channel inhibitors (e.g., Amantadine, Rimantadine) (5). However, the overuse of M2 ion channel inhibitors has led to widespread resistance in many influenza strains, complicating their clinical application (6-8). Neuraminidase inhibitors have been effective in alleviating clinical symptoms and reducing disease duration for both Influenza A and B viruses. Nevertheless, resistance to oseltamivir is increasingly reported (8) Polymerase inhibitors, such as Fluorodeoxyuridine analogues and Favipiravir, have shown potential in vitro and in vivo, though more clinical research is needed (9)

The resistance and adverse effects associated with chemical antiviral drugs have prompted a growing interest in exploring new antiviral agents, particularly herbal-based therapies (6) Punicalagin, a bioactive ellagitannin compound found in pomegranate (Punica granatum), has demonstrated antibacterial (10, 11), antiviral (5, 12-18), and anti-inflammatory properties (11, 13, 19-22) across various studies. Despite evidence supporting its anti-influenza effects, the precise mechanism by which punicalagin inhibits influenza virus replication remains unclear. Simulation studies provide comprehensive insights into drug-protein interactions, offering a pathway to further elucidate these mechanisms (Figure 1).

2. Objectives

Given the promising anti-influenza effects of punicalagin demonstrated in previous research, this study aims to deepen our understanding of its mechanism of action by evaluating its inhibitory effects on all influenza virus proteins within a simulated environment.

3. Methods

3.1. Preparation of Molecular Structures

The molecular information and two-dimensional structure of Punicalagin (PubChem CID: 348276747) were obtained from the NCBI PubChem compound database. The three-dimensional structure of Punicalagin was subsequently generated and converted into a PDB file using Avogadro software, followed by optimization and energy minimization. FASTA sequences for the proteins were retrieved from the UniProt.org server, and their PDB files were created using the I-TASSER server. Molecular docking and simulation studies were performed after the optimization and energy minimization processes.

3.2. Protein Molecular Dynamics Simulation

The molecular dynamics simulation was conducted on the PB1-F2 protein alone in water and salt to reflect changes in temperature, pressure, and a 140 mM ion concentration, achieving equilibrium. The PB1-F2 protein was modeled using Gromacs 2021 software with the G43A1 force field, and the simulation was run for 100 nanoseconds using the SPC216 water model (23). Na^+ and Cl^- ions were added to achieve the target concentration of 140 mM. Energy minimization and simulation were carried out using the steepest descent method, integrating over 50,000 steps. The LINCS algorithm was employed for equilibration under NVT and NPT ensembles. Structural features of the neuraminidase protein in the presence of the ligand were analyzed using the saved simulation trajectories (24). The resulting PDB file was subsequently used for molecular docking studies.

3.3. Molecular Docking

Molecular docking was conducted using AutoDock v.4.2 software on a Linux operating system. A grid box with dimensions of 1.4 × 1.8 × 1.9 nm (x × y × z) was defined for all blind docking experiments. PDBQT files were generated for Punicalagin (as the ligand) and the influenza A virus proteins. Docking was performed over 200 independent runs, and the resulting data were analyzed. Discovery Studio software was utilized to determine the frequency of interactions between the amino acid residues of the virus proteins and Punicalagin, as well as to calculate the types and numbers of amino acids involved in the binding site (25).

3.4. Molecular Dynamics Simulation of Protein-Ligand Complex

Finally, molecular dynamics simulation of the PB1-F2 protein-Punicalagin complex was conducted in an aqueous environment, alongside a simulation of the PB1-F2 protein alone without the ligand (24, 26). The simulation of the PB1-F2 protein-Punicalagin complex was performed for the protein with the lowest binding energy in the presence of the Punicalagin inhibitor. The results were compared to assess structural differences in

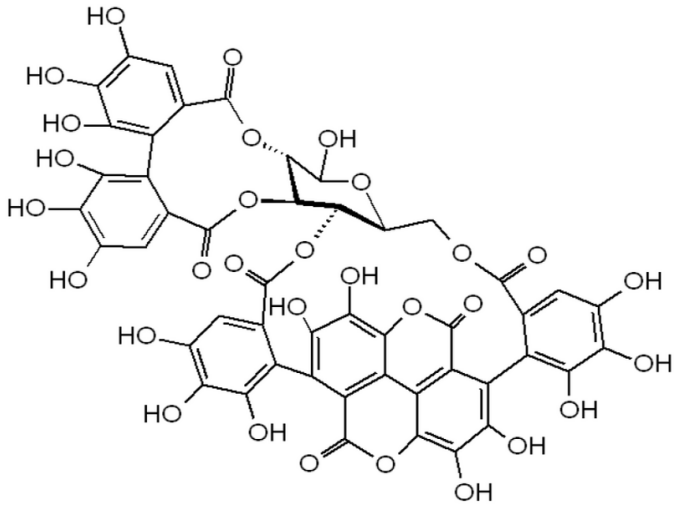

Figure 1. The chemical structure of Punicalagin

the secondary structure of the PB1-F2 protein when bound to the ligand versus when unbound. Data were extracted using Excel software and statistically analyzed using paired *t*-tests and SPSS version 22.

4. Results

4.1. Molecular Docking

Molecular docking results revealed that punicalagin exhibited a higher binding affinity for the PB1-F2 and M2 proteins (Table 1). The estimated free binding energy (BE) of punicalagin with the PB1-F2 protein was -5.76 kcal/mol, and the estimated inhibition constant (Ki) was approximately 60.13 µM (Table 1 and Figure 2). This low binding energy, coupled with a significant number of interactions and a relatively low drug concentration, indicates a strong affinity of punicalagin for the PB1-F2 protein's binding site.

For the M2 protein, punicalagin's binding energy (BE) was -5.10 kcal/mol, and the estimated inhibition constant (Ki) was around 182 µM (Table 1). Most interactions were localized in the C-terminal regions of the protein, with only two interactions occurring in the transmembrane domain (Table 1). These findings suggest that punicalagin has a higher affinity for the PB1-F2 protein compared to the M2 protein, as evidenced by the more favorable binding energy and lower inhibition constant associated with PB1-F2.

4.2. Molecular Dynamics

Root mean square deviation (RMSD) analysis indicated that the PB1-F2 protein reached equilibrium in its unbound state at approximately 10 nanoseconds. In contrast, the PB1-F2 protein bound to punicalagin achieved equilibrium at approximately 30 nanoseconds. The simulation system remained stable throughout the 100-nanosecond duration (Figure 3A). Radius of gyration (Rg) calculations revealed that equilibrium was maintained for the PB1-F2 protein in both its unbound state and when bound to punicalagin during the simulation. However, the Rg value decreased when the protein was bound to punicalagin, suggesting increased protein compactness and structural alterations due to binding. This compression may potentially affect the protein's function (Figure 3B).

Furthermore, the binding of punicalagin to the PB1-F2 protein led to a reduction in the number of intramolecular hydrogen bonds, which likely decreased the protein's dynamic behavior. This reduction could signify an inhibition of the protein's function (Figure 3C). Root mean square fluctuation (RMSF) analysis for individual amino acid residues showed that the binding of punicalagin resulted in reduced fluctuations in residues 15 - 34 and 70 - 80 of the PB1-F2 protein (Figure 3D). The molecular dynamics simulation data for the PB1-F2 protein are summarized in Table 2.

Table 1. Molecular Interaction of Punicalagin with Different Influenza Proteins

Variables and Proteins	UniProt ID	BE (kcal/mol)	EIC (μM)	Interaction Bonds
HA	P03452	-2.03	32750	Thr42, Ser339, Ser29, Val41, Ile337, Pro338, Asn28, Asn40, Thr30
M1	P03485	-3.78	1700	Ser161, Gin158, Ile51, Il14, Ser157, Pro16, His162, Ile154, Ser53, Thr56, Ser17
M2	P06821	-5.10	182	Gly61, Ser64, Glu66, Ser71, Gly62, Leu59, Ala27, Ile28, Gly67, Pro63, Met72, Phe55, Asn31, Asp24
NA	P03468	-4.31	688	Arg158, Ser157, Arg115, Thr65, Lys63, Asn194, Asn156, Trp61, Leu112
NP	P03466	-3.71	1920	Arg400, Gln399, Asp439, Ile406, Ser402, Arg446, Ala428, Glu443, Ala401, Ala403, Gln405, Gly404, Thr442
NS1	P03496	-4.17	874.27	Glu142, His169, Leu166, Ser165, Ser87, Thr143, Gly168, Pro167, Leu163, Pro164, Pro162, Ile145, Met98
NS2	P03508	-3.85	1510	Glu63, Leu55, Arg66, His56, Met50, Glu67, Gly70, Arg51, Glu74, Gln71, Leu58, Gln59
PA	P03433	-3.30	3780	Trp559, Leu606, Leu580, Lys583, Phe650, Gln610, Gln531, Trp646, Arg613, Val609
PB1	P03431	-4.22	813.35	Val644, Gln127, Ala140, Gly125, Ile517, Pro138, Ser515, Pro668, Met646, Ala652, Ala139, Ala643
PB1-F2	P0C0U1	-5.76	60.13	Gln19, Gln25, Lys29, Leu77, Trp80, Val76, Lys73, Ile16, Leu30, Lys20, His15, Ser12, Thr74
PB2	P03428	-2.95	6900	Ser634, Arg630, Ser635, Phe633, Ile710, Gln632, Asn711, Met631, Tyr592, Ile588

Abbreviations: FIE, final intermolecular energy (kcal/mol); BE, estimated free energy of binding (kcal/mol); EIC, estimated inhibition constant; HA, hemaglutinin; NA, neuraminidase; M, matrix protein; PA, polymerase A protein; PB, polymerase B protein; NP, nucleoprotein; NS, Non-structural protein.

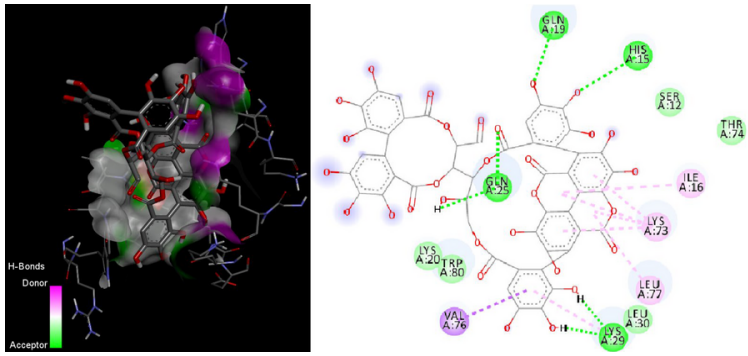

Figure 2. The structures and binding sites of Punicalagin in PB1-F2 influenza A protein and amino acid residues of proteins interacted with Punicalagin in the binding site.

Table 3 provides a detailed comparison of the secondary structural changes in the PB1-F2 protein during the 100-nanosecond simulation period, both in its unbound state and when complexed with punicalagin. The data indicate a notable reduction in the proportion of coil structures and a corresponding increase in turn structures upon binding with punicalagin. Since secondary structure plays a crucial role in maintaining protein stability and function, these alterations are likely to significantly impact the protein's activity. The observed structural changes suggest that punicalagin binding may hinder the functional efficacy of the PB1-F2 protein by inducing conformational modifications critical to its role.

5. Discussion

This study aimed to elucidate the inhibitory mechanisms of punicalagin on influenza virus proteins through molecular dynamics and docking analyses. Our findings indicate that punicalagin exhibited significant binding affinity for the PB1-F2 and M2 proteins, with the strongest inhibitory potential observed for the PB1-F2 protein. The high binding energy (BE) and low Estimated Inhibition Constant (EIC) values suggest that punicalagin binds more effectively to PB1-F2 compared to other influenza virus proteins.

PB1-F2, a short viral protein encoded by the PB1 gene, consists of approximately 90 amino acids and is divided into C-terminal (amino acids 65 - 87) and N-terminal (amino acids 1 - 37) domains (27) Previous research has highlighted PB1-F2's role in enhancing the host's inflammatory response during influenza infection through activation of the NF-κB pathway, granulocyte

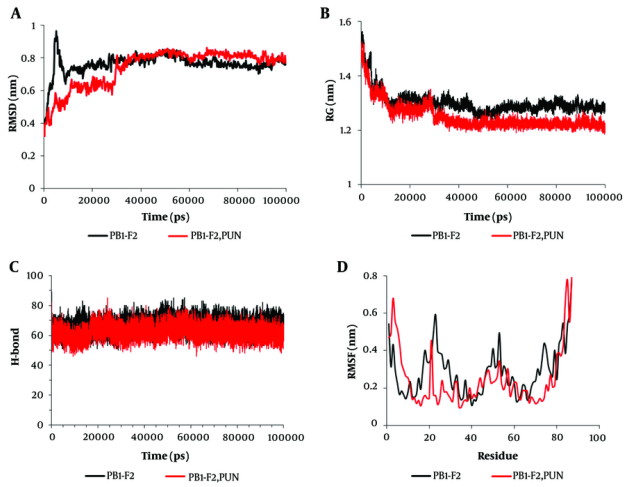

Figure 3. The amount of molecular dynamics parameters during the 100 nanoseconds of the simulation time related to the binding of punicalagin to the PB1-F2 protein. A, root Mean Square Deviations (RMSD); B, radius of gyration (Rg); C, changes in hydrogen bonds (H-bonds); D, root mean square fluctuation (RMSF). Black represents the PB1-F2 enzyme in the unbound state, while red denotes the PB1-F2 enzyme bound to punicalagin.

Table 2. Molecular Dynamics Parameters for the PB1-F2 Molecule in the States Without Binding to Punicalagin and Binding to Punicalagin [a, b]

Variables and Proteins	TE (kJ/mol)	RG (nm)	RMSD (nm)	RMSF (nm)	H-bond
PB1-F2	-253790 ± 1320	1.3 ± 0.042	0.76 ± 0.059	0.286 ± 0.13	66.6 ± 4.5
PB1-F2-punicalagin	-258055 ± 1126	1.25 ± 0.049	0.74 ± 0.11	0.246 ± 0.15	62.46 ± 4.3
P-value [c]	< 0.001	< 0.001	< 0.001	< 0.001	< 0.001

Abbreviations TE, total energy; RG, radius of gyration; RMSD, root mean square deviation of the protein skeleton.

[a] Statistical analysis was performed using a paired *t*-test.

[b] Values are expressed as mean ± SD.

[c] Compared to PB1-F2 alone with PB1-F2 and PUN complex.

chemotaxis, and apoptosis of immune cells (28) The C-terminal domain is known for its pro-inflammatory activity,(29) while the N-terminal domain contributes to increased PB1 protein expression (30) The results of our study suggest that punicalagin binds to the C-terminal region of PB1-F2, potentially inhibiting pro-inflammatory cytokine production and modulating the inflammatory response.

Punicalagin also demonstrated binding to the M2 protein, with a BE of -5.10 kcal/mol and an EIC of 182 µM. The M2 protein, a proton channel composed of four monomers, plays a crucial role in maintaining pH balance across viral membranes during entry and maturation. It is essential for viral replication and is targeted by influenza drugs such as amantadine and rimantadine (31). The interaction of punicalagin with the M2 protein involves key residues, such as Gly61, Ser64, Glu66, and Ser71 through hydrogen bonds, and Gly62, Leu59, Ala27, Ile28, Gly67, and Pro63 through hydrophobic interactions. Despite these interactions, the removal of the C-terminal helix of M2 does not significantly impact proton conduction, suggesting that punicalagin's binding may not substantially affect viral replication. However, further in vitro studies are required to confirm these findings (32, 33).

Previous studies have validated the antiviral and anti-influenza effects of pomegranate extracts and punicalagin. Sundararajan et al. reported that pomegranate polyphenols inhibit hemagglutinin and exert direct or indirect effects on the viral envelope, preventing its fusion with host cell membranes (34). Salles et al. found that pomegranate ethanol extracts and punicalagin exhibit virucidal effects against the Mayaro virus by damaging viral particles (35). Haidari et

Table 3. Secondary Structure Changes Within 100 Nanoseconds of the Simulation Time for the PB1-F2 Molecule in the State Without Binding to Punicalagin and Binding to Punicalagin

Secondary Structure	PB1-F2		PB1-F2-Punicalagin	
	Mean ± SD	%	Mean ± SD	%
Coil	15.2 ± 3.6	17.5	13.11 ± 1.4	15.1
Bend	8.36 ± 2.1	9.6	8.2 ± 2.37	9.4
Turn	11.9 ± 3.69	13.6	14.05 ± 3.5	16.2
α	51.5 ± 10.5	59.2	51.45 ± 8.1	59.27

al. demonstrated that pomegranate polyphenols inhibit hemagglutinin activity and exert direct antiviral effects (17) while Li et al. highlighted punicalagin's role in inhibiting neuraminidase (NA) activity (18).

In our study, punicalagin bound to the NA protein with a BE of -4.31 kcal/mol and an EIC of 688 µM, forming six hydrogen bonds and two hydrophobic interactions. This interaction aligns with previous findings of punicalagin's inhibitory effect on NA activity. Molecular dynamics simulations revealed significant structural changes in the PB1-F2 protein upon punicalagin binding, including alterations in its radius of gyration, secondary structure, and intramolecular hydrogen bonds. These structural modifications likely impact the protein's functionality, further supporting the potential of punicalagin as an effective antiviral agent.

Overall, the study underscores the therapeutic potential of punicalagin against influenza by targeting key viral proteins and modifying their functional dynamics. However, this research is based on in silico models, and the findings need validation through experimental studies. The predictive nature of molecular docking and dynamics simulations suggests that while punicalagin exhibits strong binding affinities, these predictions must be corroborated through biological investigations, including in vitro and in vivo experiments.

5.1. Conclusions

Punicalagin demonstrated the highest binding affinity for the PB1-F2 protein among the influenza virus proteins analyzed. Considering PB1-F2's role in amplifying inflammation during influenza infection, punicalagin may alleviate inflammation in patients by modulating the function of this protein. Furthermore, the inhibitory effect of punicalagin on PB1-F2 suggests that its anti-influenza activity could also involve inducing structural damage to the viral envelope. This dual mechanism of action underscores punicalagin's potential as a promising therapeutic agent for combating influenza.

Acknowledgements

The authors would like to express their gratitude to the Clinical Biochemistry Research Center at Shahrekord University of Medical Sciences for providing the laboratory space essential for this research.

Footnotes

Authors' Contribution: Conception: M. A. S. and M. T. M.; Design: D. A. and J. S. C.; Supervision: M. T. M.; Data collection and/or processing: J. S. C. and A. H. J.; Analysis and/or interpretation: J. S. C. and A. H. J.; Writing: M. A. S., D. A., A. H. J., J. S. C., and M. T. M.; Review and final revision approval: All authors.

Conflict of Interests Statement: The authors declared no conflict of interests.

Data Availability: The data used in the present study are available from the corresponding authors upon reasonable request.

Ethical Approval: The study was reviewed and approved by the Ethics Committee at Shahrekord University of Medical Sciences (Approval ID: IR.SKUMS.REC.1401.115).

Funding/Support: This research was supported by grant No. 6355 from Shahrekord University of Medical Sciences, Shahrekord, Iran.

References

1. Paget J, Spreeuwenberg P, Charu V, Taylor RJ, Iuliano AD, Bresee J, et al. Global mortality associated with seasonal influenza epidemics: New burden estimates and predictors from the GLaMOR Project. *J Glob Health*. 2019;**9**(2):20421. [PubMed ID: 31673337]. [PubMed Central ID: PMC6815659]. https://doi.org/10.7189/jogh.09.020421.
2. Noda T, Sugita Y, Aoyama K, Hirase A, Kawakami E, Miyazawa A, et al. Three-dimensional analysis of ribonucleoprotein complexes in influenza A virus. *Nat Commun*. 2012;**3**:639. [PubMed ID: 22273677]. [PubMed Central ID: PMC3272569]. https://doi.org/10.1038/ncomms1647.

3. Vahey MD, Fletcher DA. Low-Fidelity Assembly of Influenza A Virus Promotes Escape from Host Cells. *Cell*. 2019;**176**(3):678. [PubMed ID: 30682375]. [PubMed Central ID: PMC6498858]. https://doi.org/10.1016/j.cell.2019.01.009.
4. Palese P, Shaw ML. *Orthomyxoviridae*. Philadelphia, USA: Lippincott Williams & Wilkins, Wolters Kluwer Business; 2007.
5. Liu C, Cai D, Zhang L, Tang W, Yan R, Guo H, et al. Identification of hydrolyzable tannins (punicalagin, punicalin and geraniin) as novel inhibitors of hepatitis B virus covalently closed circular DNA. *Antiviral Res*. 2016;**134**:97-107. [PubMed ID: 27591143]. [PubMed Central ID: PMC5653380]. https://doi.org/10.1016/j.antiviral.2016.08.026.
6. Liu Q, Liu DY, Yang ZQ. Characteristics of human infection with avian influenza viruses and development of new antiviral agents. *Acta Pharmacol Sin*. 2013;**34**(10):1257-69. [PubMed ID: 24096642]. [PubMed Central ID: PMC3791557]. https://doi.org/10.1038/aps.2013.121.
7. Asadi-Samani M, Moradi MT, Bahmani M, Shahrani M. Antiviral medicinal plants of Iran: A review of ethnobotanical evidence. *Int J PharmTech Res*. 2016;**9**(5):427-34.
8. Fiore AE, Fry A, Shay D, Gubareva L, Bresee JS, Uyeki TM, et al. Antiviral agents for the treatment and chemoprophylaxis of influenza—recommendations of the Advisory Committee on Immunization Practices (ACIP). *MMWR Recomm Rep*. 2011;**60**(1):1-24.
9. Kumaki Y, Day CW, Smee DF, Morrey JD, Barnard DL. In vitro and in vivo efficacy of fluorodeoxycytidine analogs against highly pathogenic avian influenza H5N1, seasonal, and pandemic H1N1 virus infections. *Antiviral Res*. 2011;**92**(2):329-40. [PubMed ID: 21925541]. [PubMed Central ID: PMC3216401]. https://doi.org/10.1016/j.antiviral.2011.09.001.
10. Li G, Yan C, Xu Y, Feng Y, Wu Q, Lv X, et al. Punicalagin inhibits Salmonella virulence factors and has anti-quorum-sensing potential. *Appl Environ Microbiol*. 2014;**80**(19):6204-11. [PubMed ID: 25085489]. [PubMed Central ID: PMC4178673]. https://doi.org/10.1128/AEM.01458-14.
11. Ismail T, Sestili P, Akhtar S. Pomegranate peel and fruit extracts: a review of potential anti-inflammatory and anti-infective effects. *J Ethnopharmacol*. 2012;**143**(2):397-405. [PubMed ID: 22820239]. https://doi.org/10.1016/j.jep.2012.07.004.
12. Traboulsi H, Cloutier A, Boyapelly K, Bonin MA, Marsault E, Cantin AM, et al. The Flavonoid Isoliquiritigenin Reduces Lung Inflammation and Mouse Morbidity during Influenza Virus Infection. *Antimicrob Agents Chemother*. 2015;**59**(10):6317-27. [PubMed ID: 26248373]. [PubMed Central ID: PMC4576023]. https://doi.org/10.1128/AAC.01098-15.
13. Houston DMJ, Bugert JJ, Denyer SP, Heard CM. Potentiated virucidal activity of pomegranate rind extract (PRE) and punicalagin against Herpes simplex virus (HSV) when co-administered with zinc (II) ions, and antiviral activity of PRE against HSV and aciclovir-resistant HSV. *PLoS One*. 2017;**12**(6). e0179291. [PubMed ID: 28665969]. [PubMed Central ID: PMC5493292]. https://doi.org/10.1371/journal.pone.0179291.
14. Jurenka J. Therapeutic applications of pomegranate (Punica granatum L.): a review. *Alternative Med Rev*. 2008;**13**(2).
15. Reddy BU, Mullick R, Kumar A, Sudha G, Srinivasan N, Das S. Small molecule inhibitors of HCV replication from pomegranate. *Sci Rep*. 2014;**4**:5411. [PubMed ID: 24958333]. [PubMed Central ID: PMC4067622]. https://doi.org/10.1038/srep05411.
16. Yang Y, Xiu J, Zhang L, Qin C, Liu J. Antiviral activity of punicalagin toward human enterovirus 71 in vitro and in vivo. *Phytomedicine*. 2012;**20**(1):67-70. [PubMed ID: 23146421]. https://doi.org/10.1016/j.phymed.2012.08.012.
17. Haidari M, Ali M, Ward Casscells S3, Madjid M. Pomegranate (Punica granatum) purified polyphenol extract inhibits influenza virus and has a synergistic effect with oseltamivir. *Phytomedicine*. 2009;**16**(12):1127-36. [PubMed ID: 19586764]. https://doi.org/10.1016/j.phymed.2009.06.002.
18. Li P, Du R, Chen Z, Wang Y, Zhan P, Liu X, et al. Punicalagin is a neuraminidase inhibitor of influenza viruses. *J Med Virol*. 2021;**93**(6):3465-72. [PubMed ID: 32827314]. https://doi.org/10.1002/jmv.26449.
19. Xu X, Yin P, Wan C, Chong X, Liu M, Cheng P, et al. Punicalagin inhibits inflammation in LPS-induced RAW264.7 macrophages via the suppression of TLR4-mediated MAPKs and NF-kappaB activation. *Inflammation*. 2014;**37**(3):956-65. [PubMed ID: 24473904]. https://doi.org/10.1007/s10753-014-9816-2.
20. Peng J, Wei D, Fu Z, Li D, Tan Y, Xu T, et al. Punicalagin ameliorates lipopolysaccharide-induced acute respiratory distress syndrome in mice. *Inflammation*. 2015;**38**(2):493-9. [PubMed ID: 25005005]. https://doi.org/10.1007/s10753-014-9955-5.
21. Aghaei F, Moradi MT, Karimi A. Punicalagin inhibits pro-inflammatory cytokines induced by influenza A virus. *European J Integrative Med*. 2021;**43**. https://doi.org/10.1016/j.eujim.2021.101324.
22. BenSaad LA, Kim KH, Quah CC, Kim WR, Shahimi M. Anti-inflammatory potential of ellagic acid, gallic acid and punicalagin A&B isolated from Punica granatum. *BMC Complement Altern Med*. 2017;**17**(1):47. [PubMed ID: 28088220]. [PubMed Central ID: PMC5237561]. https://doi.org/10.1186/s12906-017-1555-0.
23. Saffari-Chaleshtori J, Heidari-Sureshjani E, Moradi F, Jazi HM, Heidarian E. The Study of Apoptosis-inducing Effects of Three Pre-apoptotic Factors by Gallic Acid, Using Simulation Analysis and the Comet Assay Technique on the Prostatic Cancer Cell Line PC3. *Malays J Med Sci*. 2017;**24**(4):18-29. [PubMed ID: 28951686]. [PubMed Central ID: PMC5609686]. https://doi.org/10.21315/mjms2017.24.4.3.
24. Project E, Nachliel E, Gutman M. Force field-dependent structural divergence revealed during long time simulations of Calbindin d9k. *J Comput Chem*. 2010;**31**(9):1864-72. [PubMed ID: 20033912]. https://doi.org/10.1002/jcc.21473.
25. van der Spoel D, Berendsen HJ. Molecular dynamics simulations of Leu-enkephalin in water and DMSO. *Biophys J*. 1997;**72**(5):2032-41. [PubMed ID: 9129806]. [PubMed Central ID: PMC1184398]. https://doi.org/10.1016/S0006-3495(97)78847-7.
26. Farhadian S, Heidari-Soureshjani E, Hashemi-Shahraki F, Hasanpour-Dehkordi A, Uversky VN, Shirani M, et al. Identification of SARS-CoV-2 surface therapeutic targets and drugs using molecular modeling methods for inhibition of the virus entry. *J Mol Struct*. 2022;**1256**:132488. [PubMed ID: 35125515]. [PubMed Central ID: PMC8797986]. https://doi.org/10.1016/j.molstruc.2022.132488.
27. Hai R, Schmolke M, Varga ZT, Manicassamy B, Wang TT, Belser JA, et al. PB1-F2 expression by the 2009 pandemic H1N1 influenza virus has minimal impact on virulence in animal models. *J Virol*. 2010;**84**(9):4442-50. [PubMed ID: 20181699]. [PubMed Central ID: PMC2863736]. https://doi.org/10.1128/JVI.02717-09.
28. Le Goffic R, Leymarie O, Chevalier C, Rebours E, Da Costa B, Vidic J, et al. Transcriptomic analysis of host immune and cell death responses associated with the influenza A virus PB1-F2 protein. *PLoS Pathog*. 2011;**7**(8). e1002202. [PubMed ID: 21901097]. [PubMed Central ID: PMC3161975]. https://doi.org/10.1371/journal.ppat.1002202.
29. McAuley JL, Chipuk JE, Boyd KL, Van De Velde N, Green DR, McCullers JA. PB1-F2 proteins from H5N1 and 20 century pandemic influenza viruses cause immunopathology. *PLoS Pathog*. 2010;**6**(7). e1001014. [PubMed ID: 20661425]. [PubMed Central ID: PMC2908617]. https://doi.org/10.1371/journal.ppat.1001014.
30. Kosik I, Krejnusova I, Bystricka M, Polakova K, Russ G. N-terminal region of the PB1-F2 protein is responsible for increased expression of influenza A viral protein PB1. *Acta Virol*. 2011;**55**(1):45-53. [PubMed ID: 21434704]. https://doi.org/10.4149/av_2011_01_45.

31. Pielak RM, Chou JJ. Influenza M2 proton channels. *Biochim Biophys Acta*. 2011;**1808**(2):522-9. [PubMed ID: 20451491]. [PubMed Central ID: PMC3108042]. https://doi.org/10.1016/j.bbamem.2010.04.015.
32. Cross TA, Dong H, Sharma M, Busath DD, Zhou HX. M2 protein from influenza A: from multiple structures to biophysical and functional insights. *Curr Opin Virol*. 2012;**2**(2):128-33. [PubMed ID: 22482709]. [PubMed Central ID: PMC3322387]. https://doi.org/10.1016/j.coviro.2012.01.005.
33. Liang R, Swanson JMJ, Madsen JJ, Hong M, DeGrado WF, Voth GA. Acid activation mechanism of the influenza A M2 proton channel. *Proc Natl Acad Sci U S A*. 2016;**113**(45):E6955-64. [PubMed ID: 27791184]. [PubMed Central ID: PMC5111692]. https://doi.org/10.1073/pnas.1615471113.
34. Sundararajan A, Ganapathy R, Huan L, Dunlap JR, Webby RJ, Kotwal GJ, et al. Influenza virus variation in susceptibility to inactivation by pomegranate polyphenols is determined by envelope glycoproteins. *Antiviral Res*. 2010;**88**(1):1-9. [PubMed ID: 20637243]. [PubMed Central ID: PMC7114265]. https://doi.org/10.1016/j.antiviral.2010.06.014.
35. Salles TS, Meneses MDF, Caldas LA, Sa-Guimaraes TE, de Oliveira DM, Ventura JA, et al. Virucidal and antiviral activities of pomegranate (Punica granatum) extract against the mosquito-borne Mayaro virus. *Parasit Vectors*. 2021;**14**(1):443. [PubMed ID: 34479605]. [PubMed Central ID: PMC8414858]. https://doi.org/10.1186/s13071-021-04955-4.